IJFANS INTERNATIONAL JOURNAL OF FOOD AND NUTRITIONAL SCIENCES
ISSN PRINT 2319 1775 Online 2320 7876
 UGC CARE Listed (Group -I) Journal Volume 11, Iss 11, Dec 2022

Sensitiveness of Propagation Characteristics of HermiteCosh Gaussian Laser Beams on Decentered Parameter Dependent Initial Minimum Beam Radius In The Interaction With Collisionless Magnetized Plasma

T. U. Urunkar[1] S I. Inamdar [2] M.V.Takale3, S.D.Patil[4]

[1,2]Department of Physics, Vivekanad College (Autonomous), Kolhapur 416 001, India.

[3]Department of Physics, Shivaji University, Kolhapur 416 004, India

[4]Department of Physics, Devchand College, Arjunnagar, Kolhapur 591 237, India.

Email : mvtphyunishivaji@gmail.com (M.V.Takale)

Abstract:

It is widely known that decentered parameter dependent Initial beam radius plays an important role in propagation characteristics of Hermite cosh Gaus- sian (HChG) mode laser beams in collisionless magnetized plasma by considering ponderomotive nonlinearity. The standard parabolic equation approach under WKB and paraxial approximation is utilized to investigate propagation char-acteristics of HChG laser beams in collisionless magnetised plasma. The main thrust of present paper lies on analytical investigation of numerical interval and turning points of decentered parameter dependent Initial beam radius which governs self-focusing and defocusing of HChG laser beams. Eventually results are discussed in the light of numerical intervals and turning points of initialbeam radius.

Keywords: Self-focusing, Hermite cosh-Gaussian beam, decentered parameter, magnetized plasma, initial beam radius.

Introduction:

The interaction of laser radiations with plasma gives various nonlinear phe- nomena such as, self-phase modulation, self-focusing, harmonic generation etc. [1-3]. Investigation of these nonlinear phenomena has been a subject of exper- imental and theoretical research due to their vast applications in laser driven fusion [4], laser based electron accelerators [5,6], X-ray lasers [7], fast ignition for inertial confinement fusion (ICF) [8]. For these applications it is necessaryto propagate the laser beam without any divergence and by maintaining a good plasma interaction.

The self- focusing is a genuinely nonlinear phenomenon caused by nonlin-ear response of material medium prompting its reformed refractive index. In the laser-plasma-interaction, the self-focusing concerning the laser beams [9-11] has been the focal point of consideration as it influences some other nonlinear phenomena. Theoretical and experimental investigations on propagation char- acteristics of different laser beam profiles such as Gaussian [12], cosh-Gaussian (ChG) [13,14], Hermite cosh-Gaussian (HChG) [15,16], elliptical Gaussian [17], and

hollow Gaussian beams [18] have been reported in recent years.

Theoretical researchers have recently focused their attention on the parax- ial wave family of laser beams. The HChG beam is one of the solutions tothe paraxial wave equation, and it is created in the lab by superimposing two decentered HChG beams as Cosh-Gaussian ones [19]. Under Wentzel-Kramers- Brillouin (WKB) and paraxial approximations, the present theoretical analysis uses a parabolic equation technique. According to a review of the literature, the decentered parameter[20,21] and the initial beam radius [14, 22, 23] are impor- tant factors in the self-focusing phenomena. However, in present paper we have emphasized analytically to set the numerical interval of decentered parameter dependent initial minimum beam radius for various nonlinear phenomena such as self-focusing, self-trapping, and defocusing. We have explored the effect of intersecting points initial minimum beam radius on self-focusing and defocusing of HChG laser beam.

This paper is organised in the following way: Section. 2 gives the beam width parameter differential equation of the HChG laser beam propagating through a collisionless magnetized plasma for mode indices values m = 0, 2, and 4. In section 3, analytical investigation is graphically discussed in detail. In section4, a brief conclusion is included.

2. Theoretical Framework

Let us consider the propagation of HChG laser beam through a collisionless magnetized plasma along the z direction along which static magnetic field B_0 is applied. The electric field of the laser beam propagating in either modes i.e.in E and O modes can be written as [24],

$$E_{\pm} = xE_{0\pm}(r, z)exp[-i(\omega t - k_{\pm}z)] \quad (1)$$

where is $k_{\pm}\frac{\omega}{c}\sqrt{\varepsilon_{\pm}}$ the propagation constant of the wave where $\varepsilon_{\pm}$ is the effective dielectric constant of magnetized plasma, ω is frequency of laser used and c is the speed of light in vacuum.

$$\varepsilon_{\pm} = \varepsilon_{0\pm} + \varphi_{\pm}(E_{\pm}E^{*}) \quad (2)$$

where $\varepsilon_{0\pm}$ and $\varphi_{\pm}(E_{\pm}E^{*})$ are the linear and nonlinear parts of the dielectric constant of collisionless magnetized plasma and can be expressed as,

$$\varepsilon_{0\pm} = 1 - \frac{\omega_p^2}{\omega(\omega \mp \omega_c)} \quad (3)$$

$$\varphi_{\pm}\left(E_{\pm}E_{\pm}^{*}\right) = \frac{\omega_p^2}{\omega(\omega \mp \omega_c)}\left[1 - exp\left(-\alpha E_{\pm}E_{\pm}^{*}\right)\right] \quad (4)$$

Here, $\omega_p = (4\pi N_0 e^2/m)^{1/2}$ is the plasma frequency and $\omega_c = eB_0/mc$ is cyclotron frequency.

e and m are the electronic charge and its rest mass respectively.

In the light of Maxwells elctrodynamic equations, the general form of wave equation governing the propagation of laser beam is given as,

$$\frac{\partial^2 E_\pm}{\partial z^2} + \delta_\pm \left(\frac{\partial^2 E_\pm}{\partial r^2} + \frac{1}{r}\frac{\partial E_\pm}{\partial r}\right) + \frac{\omega^2}{c^2}(\varepsilon_\pm E_\pm) = 0 \quad (5)$$

Where, $\delta_\pm = \frac{1}{2}\left(1 \mp \frac{\varepsilon_{0\pm}}{\varepsilon_{0zz}}\right)$ and $\varepsilon_{0zz} = 1 - \frac{\omega_p^2}{\omega^2}$

The electric field $E_\pm$ given by Eq. (1) satisfies Eq.(5). In circular cylindrical coordinate system, under slowly varying envelope approximation, the evolution of electric field envelope in collisionless magnetized plasma can be expressed as,

$$-2ik_\pm \frac{\partial E_\pm}{\partial z} + \delta_\pm \left(\frac{\partial^2 E_\pm}{\partial r^2} + \frac{1}{r}\frac{\partial E_\pm}{\partial r}\right) + \frac{\omega^2}{c^2}\varphi_\pm\left(E_\pm E_\pm^*\right) = 0 \quad (6)$$

In WKB approximation one can neglect $\partial^2 E_\pm/\partial z^2$ in Eq. (5). The complex amplitude of electric vector may be expressed as,

$$E_{0\pm}(r, z) = A_\pm(r, z) exp[-ik_\pm(z) S_\pm(r, z)] \quad (7)$$

where, $A_\pm(r, z)$ and $S_\pm(r, z)$ are real functions of r and z . $S_\pm$ is known as eikonal of the beam. Substituting above equation in Eq. (6) and separating real and imaginary parts of resulting equations one obtains,

$$2\left(\frac{\partial S_\pm}{\partial z_\pm}\right) + \delta_\pm \left(\frac{\partial S_\pm}{\partial r}\right)^2 + \frac{2S_\pm}{k_\pm}\frac{\partial k_\pm}{\partial z_\pm} = \frac{\delta_\pm}{k_\pm^2 A_\pm}\left(\frac{\partial^2 A_\pm}{\partial r^2} + \frac{1}{r}\frac{\partial A_\pm}{\partial r}\right) + \frac{\omega^2}{c^2}\varphi_\pm\left(A_\pm A_\pm^*\right) \quad (8)$$

$$\frac{\partial A_\pm^2}{\partial z} + \delta_\pm \frac{\partial S_\pm}{\partial r}\frac{\partial A_\pm^2}{\partial r} + \delta_\pm A_\pm^2\left(\frac{\partial^2 S_\pm}{\partial r^2} + \frac{1}{r}\frac{\partial S_\pm}{\partial r}\right) + \frac{A_\pm^2}{k_\pm}\frac{\partial k_\pm}{\partial z} = 0 \quad (9)$$

Following approach given by Akhmanov *et.al.* [25] and developed by Sodha *et.al.* [26], the solution of Eqs. (8) and (9) for HChG laser beam can be written as

$$A_\pm^2 = I\, exp\left[-2\left(\frac{r}{f_\pm r_0} + \frac{b}{2}\right)^2\right] + \left[-2\left(\frac{r}{f_\pm r_0} - \frac{b}{2}\right)^2\right] + 2I\left[-2\left(\frac{r}{f_\pm r_0} + \frac{b}{2}\right)^2\right] \quad (10)$$

Where, $I = H_m^2 \frac{E_{0\pm}^2}{f_{0\pm}^2} \exp\left(\frac{b^2}{2}\right)$

$$S_\pm = \frac{r^2}{2}\beta_\pm(z) + \varphi_\pm(z) \quad (11)$$

$$\beta_\pm(z) = \frac{1}{\delta_\pm}\frac{1}{f_\pm}\frac{df_\pm}{dz} \quad (12)$$

Where, $E_{0\pm}^2$ is an axial laser intensity and $f_\pm$ is the dimensionless beam width parameter for E and O modes respectively. ${\beta_\pm}^2$ gives the radius of the curvature of wave front and $\varphi_\pm(z)$ is known as phase. Substituting Eqs.(10), (11) and (12) in Eq. (8) and equating coefficients of r^2 on both sides we get,

For $m = 0$

$$\frac{\partial^2 f_\pm}{\partial \xi_\pm^2} = \frac{1}{\varepsilon_{0\pm}}\frac{1}{f_\pm^3}\left\{\frac{(12-12b^2-b^4){\delta_\pm}^2}{3} - \frac{(2-b^2)\exp[-p_\pm]p_\pm\rho_\pm^2\gamma_\pm\delta_\pm}{2}\right\} \quad (13)$$

For $m = 2$

$$\frac{\partial^2 f_\pm}{\partial \xi_\pm^2} = \frac{1}{\varepsilon_{0\pm}}\frac{1}{f_\pm^3}\left\{-\frac{(84+60b^2-b^4){\delta_\pm}^2}{3} + \frac{2(b^2-10)\exp[-p_\pm]p_\pm\rho_\pm^2\gamma_\pm\delta_\pm}{2}\right\} \quad (14)$$

For $m = 4$

$$\frac{\partial^2 f_\pm}{\partial \xi_\pm^2} = \frac{1}{\varepsilon_{0\pm}} \frac{1}{f_\pm^3} \left\{ \frac{(308+108\, b^2-b^4)\delta_\pm{}^2}{3} + \frac{72(b^2-18)\exp[-p_\pm] p_\pm \rho_\pm^2 \gamma_\pm \delta_\pm}{2} \right\} \qquad (15)$$

Where, $\gamma_\pm = \frac{\Omega_p^2}{1\mp\Omega_c}$, $\Omega_p = \frac{\omega_p}{\omega}$, $\Omega_c = \frac{\omega_c}{\omega}$, $p_\pm = \frac{\alpha E_{0\pm}^2}{f_\pm^2}$, $\rho_\pm = \frac{r_0 \omega}{c}$

The quantity $p_\pm$ which is dimensionless and proportional to $E_{0\pm}^2$represents the dimensionless beam power on a suitably chosen scale. The beam width parameters $f_\pm$ is a function of $\xi_\pm$, here $\xi_\pm = z/k_\pm r^2$ is the normalized propagation distance.

1. Results and Discussion

Equations (13)-(15) are second order nonlinear differential equations which gives variation of $f_\pm$ with $\xi_\pm$ for $m = 0$, $m = 2$, $m = 4$ respectively .The first term on the right-hand side gives diffraction divergence of the beam and the second term gives to the convergence of beam which results from the nonlinearityin dielectric constant of collisionless magnetized plasma.

Under initial condition (at $\xi_\pm = 0, f_{\pm=1}$) the general power of laser beam p_+ and beam radius ρ_+ are replaced by initial power p_{0+} and initial beam radius ρ_{0+}. Consider m = 0 mode for further investigation. For initial condition one may obtain equation of initial curve [50-52].

$$\rho_{0\pm}^2 = \frac{2}{3}\frac{\delta_\pm}{\gamma_\pm} \frac{\exp[-p_{0\pm}]}{p_{0\pm}} \frac{(b^4+12b^2-12)}{(b^2-2)} \qquad (16)$$

Here, $\rho_{0\pm}$ represent initial beam radius coresponding to E and O modes. Only E mode is subject to the following investigation.

By following similar process given by Valkunde et.al.[27] one may obtain value of initial beam power p_{0+} = 1 for initial minimum beam radius ρ_{0+min}. By using numerical values N_0 = $1 \times 10^{18} cm^{-3}$, $\omega = 1.776 \times 10^{15} rad/s$, $B_0 = 10^6 gauss$ equation (16) gives,

$$\rho_{0+min} = 42.1483 \left(\frac{(b^4+12b^2-12)}{(b^2-2)}\right)^2 \qquad (17)$$

From Eq.(17) it is seen that ρ_{0+min} is purely b dependent. By using numer- ical computation under the condition that $\rho_{0+min} > 0$ one may obtain domain of decentered parameter. Figure 1 throws light on domain of decentered param- eter for mode index m=0. Form Figure 1. it is seen that as initially as value of decentered parameter b increases the value of ρ_{0+min} decreases and by using simple mathematical calculation one may show that ρ_{0+min} has minimum value ρ_{0+min}= 206.515 at b = 2.4850 . After reaching minimum value of ρ_{0+min} withincrease in value of decentered parameter b value of ρ_{0+min}increases.

Hence the above main domain is further divided into two sub domains

$1.4142 \le b \le 2.4850$ and $b \ge 2.4850$.

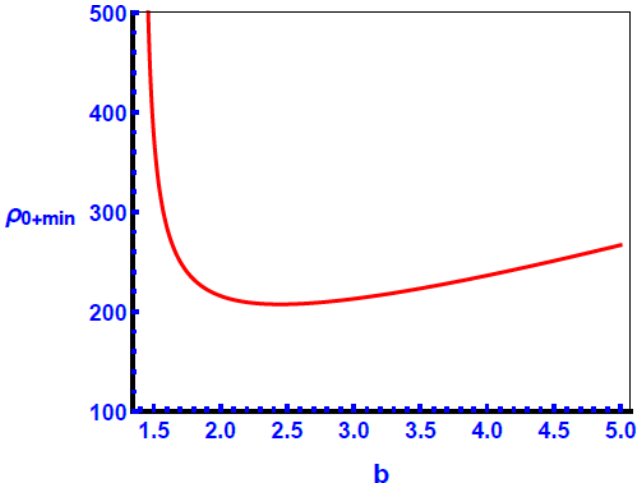

Figure 1: Variation of ρ_{0+min} with decentered parameter b for mode index m=0.

Under initial condition (at $\xi = 0$, $f = 1$), $\frac{\partial^2 f_{\pm}}{\partial \xi_{\pm}^2} = 0$ and for $p_{0+} = 1$ the right-hand side of the Eq. (13) is represented by function $F(\rho_{0+min})$ with value of decentered parameter b from $1.4142 \leq b \leq 2.4850$ and $b \geq 2.4850$.

$$F(\rho_{0+min}) = -0.33333\,(12 - 12b^2 - b^4) + 0.000146513 \quad (18)$$

To explore effect of initial minimum beam radius right at the beginning one needs to give careful attention on plots shown in Figures 2a and 2b given here.

The plots shown in Figures 2a and 2b can be examined for three distinct conditions for propagation characteristics expressed follows and the simple an- alytical approach prompts following limits for initial minimum beam radius,

For Figure 2a ($1.4142 \leq b \leq 2.4850$ **)**

For Self-trapping

$$F(\rho_{0+min}) = 0 \text{ for } \rho_{0+min} = 427.291 \text{ (b = 1.5)}$$
$$\text{for } \rho_{0+min} = 261.876 \text{ (b = 1.8)}$$
$$\text{for } \rho_{0+min} = 238.724 \text{ (b = 2.1)}$$

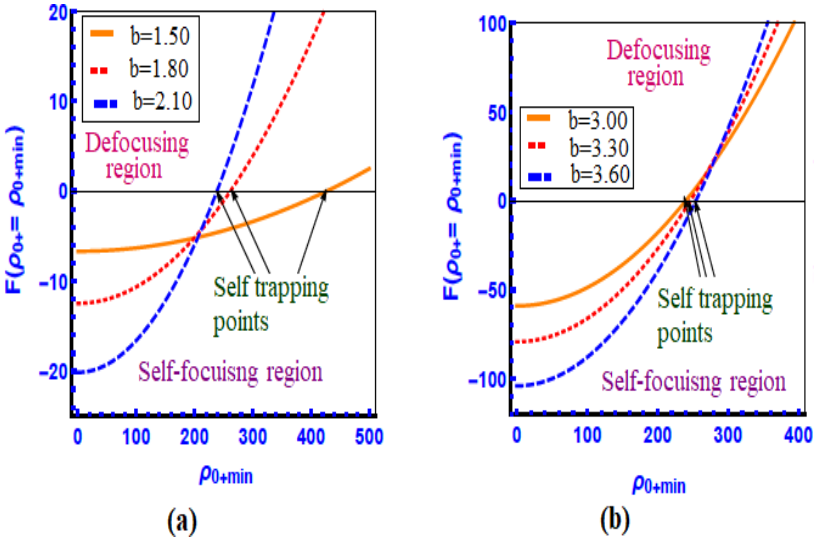

Figure 2: Graph of $F(\rho_{0+min})$ against ρ_{0+min} for mode index m=0 (a) for $1.4142 \leq b \leq 2.4850$, (b) for $b \geq 2.4850$.

For Self-focusing:

For Defocusing

$$F(\rho_{0+min}) < 0 \text{ for } \rho_{0+min} \leq 238.724$$

$$F(\rho_{0+min}) > 0 \text{ for } \rho_{0+min} \geq 427.29$$

For Figure 2b $(b \geq 2.4850)$

For Self-trapping

$$F(\rho_{0+min}) = 0 \text{ for } \rho_{0+min} = 239.851 \ (b = 3.0)$$
$$\text{and for } \rho_{0+min} = 246.419 \ (b = 3.3)$$
$$\text{and for } \rho_{0+min} = 254.28 \ (b = 3.6)$$

For Self-focusing:

$$F(\rho_{0+min}) < 0 \text{ for } \rho_{0+min} \leq 239.851$$

For Defocusing

$$F(\rho_{0+min}) > 0 \text{ for } \rho_{0+min} \geq 254.28$$

From Figure 2a (for $1.4142 \leq b \leq 2.4850$) and Figure 2b (for $b \geq 2.4850$) it is seen that for $1.4142 \leq b \leq 2.4850$, three curves intersects each other at three different points in self-focusing region where as for $b \geq 2.4850$ the three curves intersects each other at three different points in defocusing region. These intersecting points affect the propagation characteristics of laser beams through magnetised plasma. The intersecting points are as follow:

Figure 2a (for $1.4142 \leq b \leq 2.4850$**)**

$\rho_{0+min} = 199.479$ for $b = 1.50$ and $b = 1.80$

$\rho_{0+min} = 211.437$ for $b = 1.80$ and $b = 2.10$

$\rho_{0+min} = 206.0421$ for $b = 1.50$ and 2.10

Figure 2b (for $b \geq 2.4850$**)**

$\rho_{0+min} = 269.357$ for $b = 3.00$ and $b = 3.30$

$\rho_{0+min} = 285.592$ for $b = 3.30$ and $b = 3.60$

$\rho_{0+min} = 277.962$ for $b = 3.00$ and 3.60

From Figures 3a and 3b it is clear that at the turning points, for a given ρ_{0+min}, there can be two distinct values of decentered parameter b are possible which gives the identical $F(\rho_{0+min})$ value or one may also say that there can be two identical beam width parameter differential equation for two distinct values of decentered parameter b such that the evolution of laser beam would be identical. The above significance of graph is also evident from the Eq.(18) itself. In Self-focusing region of Figure 3a $\rho_{0+min} \leq 238.724$ which is the present region of interest. The Figures 4a and 4b gives variation of beam width param- eter f_+ againstnormalised

propagation distance ξ_+ before and after turning points respectively.

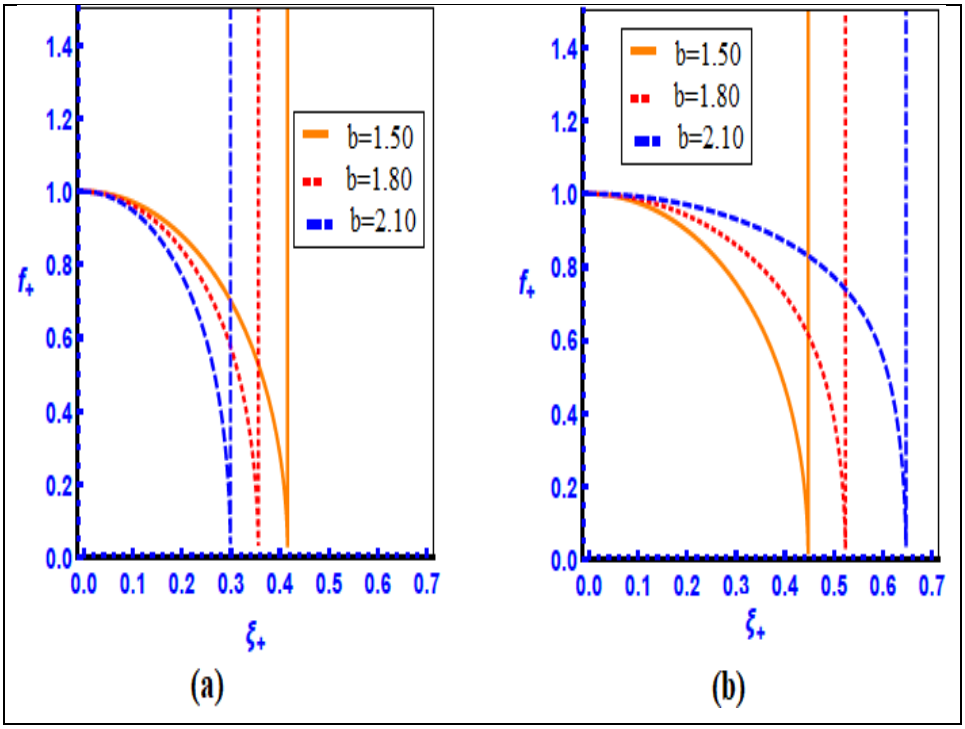

Figure 3: Graph of f_+ against ξ_+ for mode index m=0 in self focusing region of 1.4142 ≤ b ≤ 2.4850 (a) before turning points (ρ_{0+min} = 150) (b) after turning points (ρ_{0+min} = 204).

In Figures 4a and 4b strong self-focusing is observed, it also reveals that initially beam starts converging but after appreciable propagation through mag- netized plasma, the influence of diffraction divergence dominate the converging effect due to nonlinearity and beam starts diverging. However in Figure 4a ,the self-focusing length is observed over smaller interval of ξ_+ as compared the self- focusing length observed in Figure 4b over a given range of ξ_+. Additionally, with increase in values of decentered parameter, the effect of b on self-focusing length in Figure 4a is exactly opposite to that in the Figure 4b. That is from Figure 4a it is seen that with increase in a value of decentered parameter **b** self- focusing length decreases whereas from Figure 4b it is seen that with increase in a value of decentered parameter **b** self-focusing length increases.

In Defocusing region of Figure 3b $\rho_{0+min} \geq 116.386$ which is the present region of interest the Figures 5a and 5b gives variation of beam width parameter f_+ against normalized propagation distance ξ_+ before and after turning points respectively. From Figure 5a. it is seen in that before turning points, oscillatory defocusing is observed whereas after turning points steady state defocusing is observed over given range of ξ_+ as shown in Figure 5b.

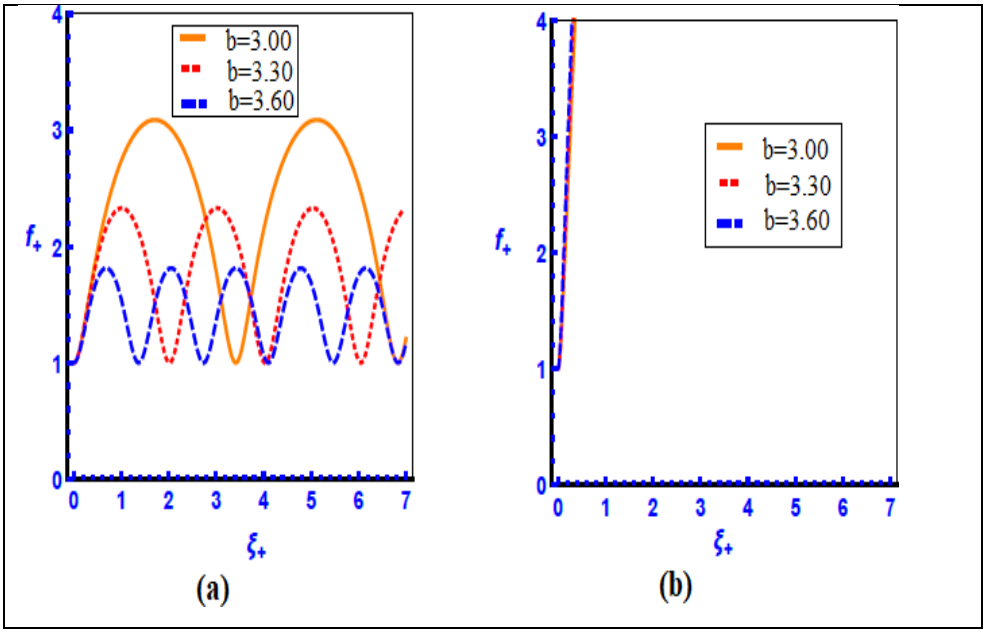

Figure 4: Graph of f_+ against ξ_+ for mode index m=0 in defocusing region of $b \geq 2.4850$ (a) before turning points ($\rho_{0+min} = 240$) (b) after turning points ($\rho_{0+min} = 400$).

A similar process is followed for a higher mode indices $m = 2$ and $m = 4$. The numerical results and the domain are shown in Table and Graphical results are shown in Figures below (for mode index $m = 2$ refer Figures 6 to 10 and formode index $m = 4$ refer Figures 11 to 15).

Numerical results for mode indices m=2 and m=4					
Mode index	Domains of b.	For Self Trapping $\rho 0+min$	For Self -focusing $\rho 0+min$	For de-focusing $\rho 0+min$	Turning points ρ_{0+min}
$m = 2$	$3.17 < b < 6.16$	175.52(b = 4.00) 144.70(b = 5.00) 139.14(b = 6.00)	< 139.14	> 175.52	119.84 (b = 4.00, 5.00) 126.19 (b = 4.00, 6.00) 131.17 (b = 5.00, 6.00)
	$b > 6.16$	145.32(b = 8.00) 151.79(b = 9.00) 159.41(b = 10.00)	< 145.32	> 159.41	170.73 (b = 8.00, 9.00) 178.47 (b = 8.00, 10.00) 185.11 (b = 9.00, 10.00)
$m = 4$	$4.24 < b < 8.29$	90.55(b = 5.0) 69.43(b = 6.0) 63.85(b = 7.0)	< 63.86	> 90.55	51.67 (b = 6.0, b = 7.0) 53.62 (b = 5.0, b = 7.0) 55.22 (b = 6.0, b = 7.0)
	$b > 8.29$	62.58(b = 9.0) 63.77(b = 10.0) 65.55(b = 11.0)	< 62.58	> 65.55	67.57 (b = 9.0, b = 10.0) 72.09 (b = 9.0, b = 11.0) 72.10 (b = 9.0, b = 11.0)

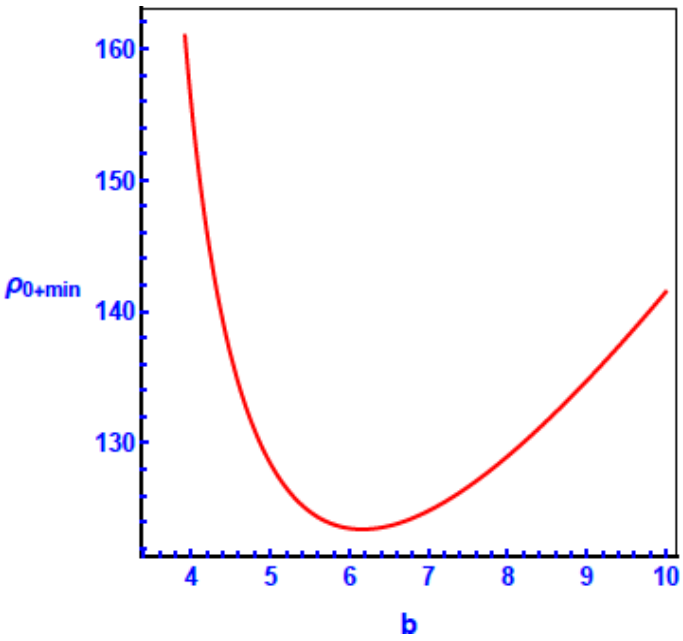

Figure 5: Variation of ρ_{0+min} with decentered parameter b for mode index $m = 2$.

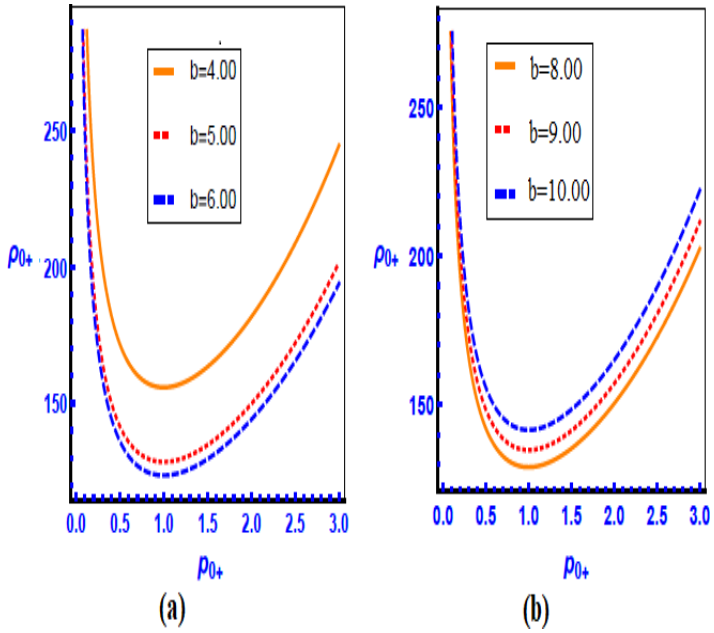

Figure 6: critical curves for mode index $m = 2$ (a) for $3.17 \leq b \leq 6.16$,(b) for $b \geq 6.16$

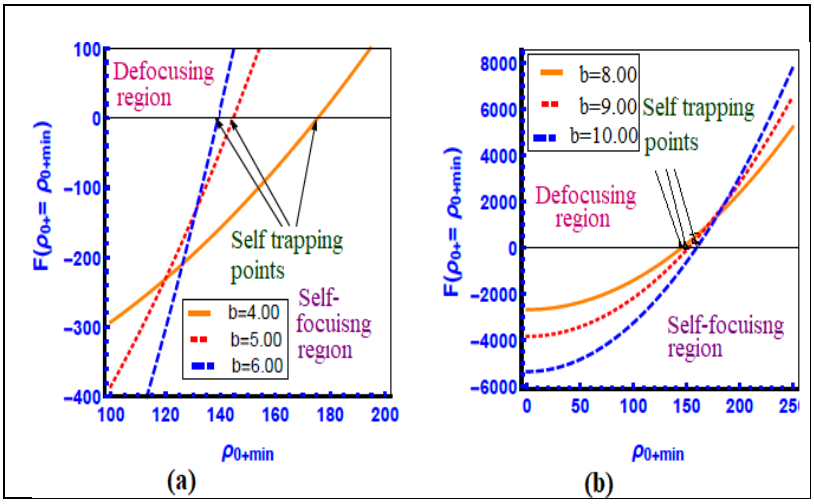

Figure 7: Graph of $F(\rho_{0+min})$ against ρ_{0+min} for mode index $m = 2$ (a) for $3.17 \leq b \leq 6.16$ (b) for $b \geq 6.16$

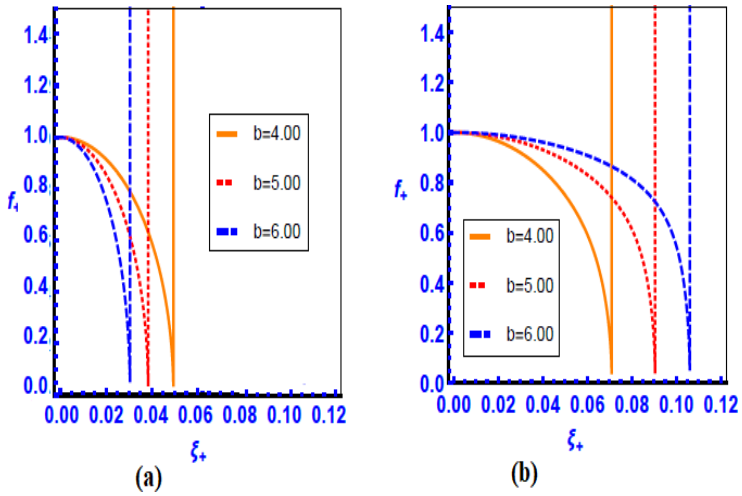

Figure 8: Graph of f_+ against ξ_+ for mode index $m = 2$ in self-focusing region of 3 ≤

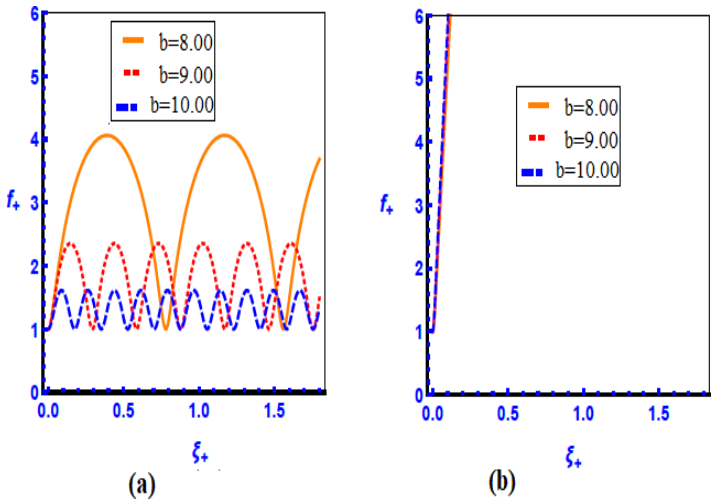

6.16 (a) before turning points ($\rho_{0+min} = 80$) (b) after turning points ($\rho_{0+min} = 135$)

Figure 9: Graph of f_+ against ξ_+ for mode index $m = 2$ in defocusing region of$b \geq 6.16$

(a)before turning points ($\rho_{0+min} = 148$) (b) after turning points ($\rho_{0+min} = 200$)

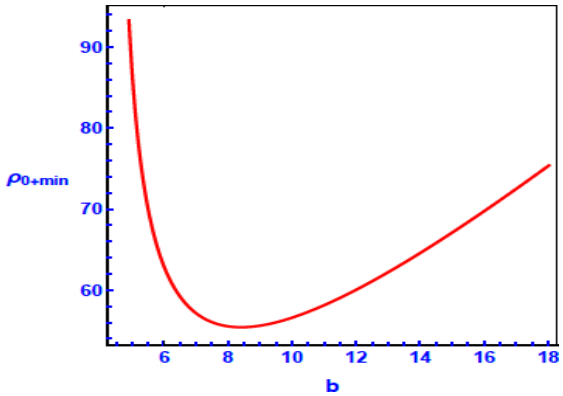

Figure 10: Variation of ρ_{0+min} with decentered parameter b for mode index $m = 4$.

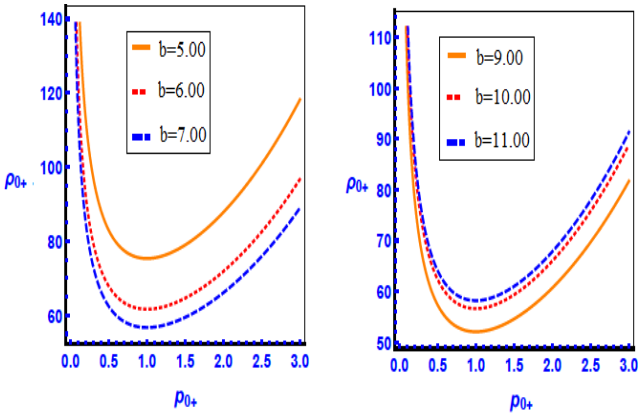

Figure 11: critical curves for mode index $m = 4$ (a) for $4.24 \le b \le 8.29$,(b) for $b \ge 8.29$

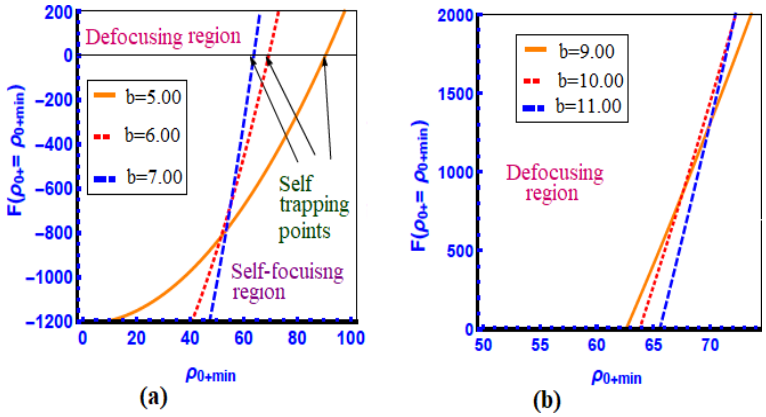

Figure 12: Graph of $F(\rho_{0+min})$ against ρ_{0+min} for mode index $m = 4$ (a) for $4.24 \le b \le 8.29$

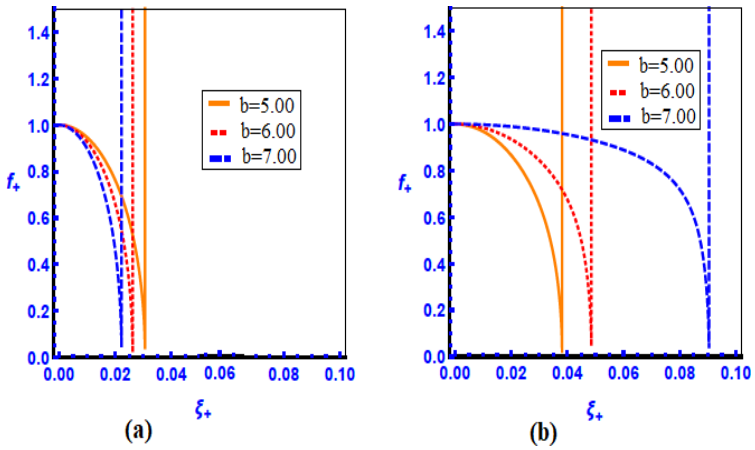

(b) for$b \geq 8.29$

Figure 13: Graph of f_+ against ξ_+ for mode index m = 4 in self-focusing region of $4.24 \leq b \leq$
8.29 (a) before turning points (ρ_{0+min} = 30) (b) after turning points (ρ_{0+min} = 56)

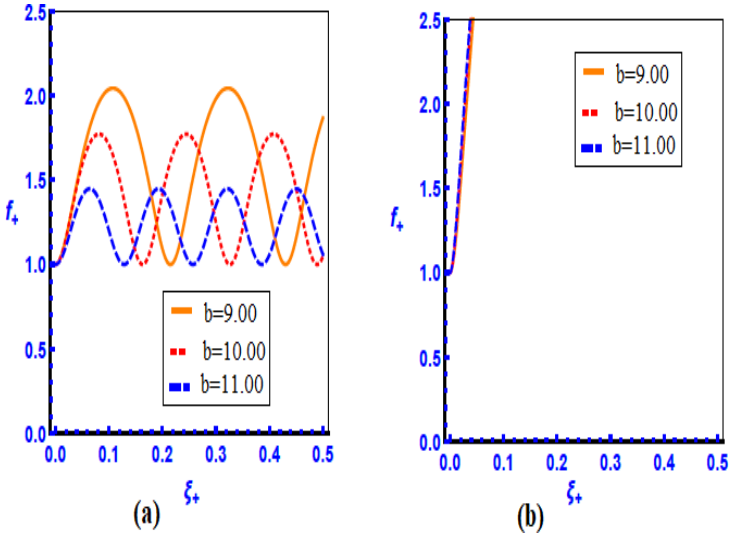

Figure 14: Graph of f_+ against ξ_+ for mode index m = 4 in self-focusing region of $b \geq$ 8.29

(a) before turning points (ρ_{0+min} = 60) (b) after turning points (ρ_{0+min} = 75)

Conclusion

In the present investigation, the domain of value of decentered parameter b for a different mode indices (m = 0, m = 2 and m = 4) as well as the numerical interval of ρ_{0+min} for a different nonlinear phenomenon such as, self- focusing, self-trapping and defocusing are obtained by using simple calculus. The following important conclusions are drawn from the present analysis:

a. For each mode index there are two domains of decentered parameter b.

b. For each domain of decentered parameter b, ρ_{0+min} show different be- haviour.

c. With the increase in the mode index of the laser beam, the values of

2. ρ_{0+min} for decentered parameter *b* decreases.

a. With increase in values of decentered parameter in Self- focusing region, exactly opposite trends of Self- focusing before and after turning points are observed . That is in Self- focusing region, self-focusing length before turning points and after turning points shows exactly opposite changes..

b. In defocusing region, different trends of defocusing (Oscillatory and Steady state defocusing) before and after turning points are observed .

3. Thus, the present analytical investigations based on decentered parameter and critical beam radius offer a choice to govern the propagation characteristics of the HChG laser beam through collisionless magnetized plasma.

References:

1. S. A. Akhmanov, A. P. Sukhorukov and R. V. Khokhlov Sov. Phys. Usp.,10 (1968) 609-636.
2. S. Vij, M. Aggarwal, , N. Kant, Opt. Commun..383(2016) 349.
3. [3]N. Kant, D.N. Gupta, and H. Suk, Phys. Lett. A 375 (2011) 31343137
4. F. Winterberg, Laser Part. Beams 26 (2008) 127.
5. H.S.Ghotra and N. Kant, Opt. Commun. 383 (2016) 169.
6. D.N. Gupta, N. Kant, D. E. Kim and H. Suk, Phys. Lett. A 368 (2007)402407
7. J. Parashar, H. D. Pandey, and V. K. Tripathi, Phys. Plasmas 4 (1997)3040.
8. H. Hora , Laser and Particle Beams 25 (2007) 37-45.
9. T. S. Gill, R. Kaur, and R. Mahajan, Phys. Plasmas 17 (2010) 093101.
10. R. Kaur, T. S. Gill, and R. Mahajan, Optik (Stuttgart)122 (2011) 375.
11. A.T. Valkunde, S.D. Patil , M.V. Takale, B.D. Vhanmore, T.U. Urunkar,
12. K.M. Gavade, D.N. Gupta, Optik 158 (2018) 1034 -1039.
13. S.D. Patil, M.V. Takale, S.T. Navare, M.B. Dongare, V.J. Fulari, Optik 124 (2013) 180- 183.
14. [13] M. Aggarwal, S. Vij, N. Kant, Optik 125 (2014) 5081-5084.
15. T. U. Urunkar, S. D. Patil, A. T. Valkunde, B. D. Vhanmore, K. M.
16. Gavade and M. V. Takale (2018) Commun. Theor. Phys. 70 220
17. A. Belafhal , M. Ibnchaikh. Opt. Commun. 186 (2000) 269-276
18. D. Zhao , H. Mao, H. Liu, J. Opt. A: Pure Appl. Opt. 6 (2004) 77-83.
19. A. Singh, M. Aggarwal, T. S. Gill, Optik 119 (2008) 559-564.
20. A.K.Shafeeque Ali, M .Lakshmanan, Phys. Lett. A 384 (2020) 126527[19] L.Baida , L. Shirong, Optik 112, No. 11 (2001) 503-506.
21. S.D. Patil, M.V. Takale, V.J. Fulari, M.B. Dongare, J Mod Opt. 21 (2008)3527-3533.

ISSN PRINT 2319 1775 Online 2320 7876
 UGC CARE Listed (Group -I) Journal Volume 11, Iss 11, Dec 2022

22. B.D. Vhanmore, S.D. Patil, A.T. Valkunde, T.U. Urunkar, K.M. Gavade,
23. M.V. Takale, Laser Part. Beams 35 (2017) 670-676.
24. A. Sharma, G. Prakash, and M. P. Verma, Phys. Plasmas, 10 (2003) 4079.
25. A. Sharma, I. Kourakis, and M. S. Sodha, Phys. Plasmas 15 (2008)103103.
26. M. Aggarwal, H. Kumar, N. Kant, Optik 127 (2016) 2212-2216.
27. S. A. Akhamanov, A. P. Sukhorov, and R. V. Khokhlov, Sov. Phys. Usp. 93 (1968) 609.
28. M. S. Sodha, A. K. Ghatak, and V. K. Tripathi, Prog. Opt. 13 (1976) 171.
29. A.T. Valkunde, S.D. Patil, B.D. Vhanmore, T.U. Urunkar, K.M. Gavade,
30. M.V. Takale, V.J. Fulari, Phys. Plasmas 25 (2018) 0331031.